PROCEEDINGS OF SCIENCE

Spanning of Topological sectors, charge and susceptibility with naive Wilson fermions

Abhishek Chowdhury, Asit K. De,* Sangita De Sarkar, A. Harindranath, Santanu Mondal, Anwesa Sarkar
Theory Division, Saha Institute of Nuclear Physics
1/AF Bidhan Nagar, Kolkata 700064, India

Jyotirmoy Maiti
Department of Physics, Barasat Government College,
10 KNC Road, Barasat, Kolkata 700124, India

We study the topological charge and the topological susceptibility in lattice QCD with two degenerate flavors of naive Wilson fermions at two values of lattice spacings and different volumes, for a range of quark masses. Configurations are generated with DDHMC/HMC algorithms and smoothened with HYP smearing. We present integrated autocorrelation time for both topological charge and topological susceptibility at the two lattice spacing values studied. The spanning of different topological sectors as a function of the hopping parameter κ is presented. The expected chiral behaviour of the topological susceptibility (including finite volume dependence) is observed.

The XXIX International Symposium on Lattice Field Theory - Lattice 2011
July 10-16, 2011
Squaw Valley, Lake Tahoe, California

*Speaker

PoS(Lattice 2011)099

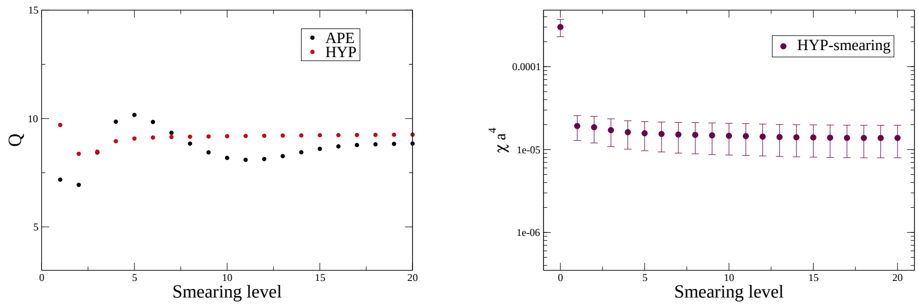

Figure 1: (a) Topological charge versus smearing levels for APE and HYP smearing at $\kappa = 0.15825$, $\beta = 5.6$ and volume $24^3 \times 48$. (b) Topological susceptibility versus HYP smearing levels at $\kappa = 0.15825$, $\beta = 5.6$ and volume $24^3 \times 48$.

1. Introduction

Earlier attempt [1] in lattice QCD to verify the suppression of topological susceptibility with decreasing quark mass (m_q) with unimproved Wilson fermions and HMC algorithm was unable to unabiguously confirm the suppression. Since topological susceptibility is a measure of the spanning of different topological sectors of QCD vacuum, the inability to reproduce the predicted suppression may raise concerns about the simulation algorithm and the particular fermion formulation to span the configuration space correctly and/or efficiently. In this work, we perform a systematic study using unimproved Wilson fermions and demonstrate the suppression of topological susceptibility with decreasing quark mass. This work is part of an ongoing program [2, 3] to study the chiral properties of Wilson lattice QCD. For details on measurements of topological charge and susceptibility, and numerical values of measured quark masses, pion masses and topological susceptibilities see Ref. [4]. Our results of the topological susceptibility favourably compare in Ref. [4] with that from a recent mixed action calculation employing clover fermions and overlap fermions for the sea and the valence sectors respectively [5]. The detailed account of low lying spectroscopy will appear separately.

2. Measurements

We have generated ensembles of gauge configurations by means of HMC [6] and DDHMC [7] algorithms using unimproved Wilson fermion and gauge actions with $n_f = 2$ mass degenerate quark flavours at two values of the gauge coupling (β =5.6, 5.8) . At $\beta = 5.6$ the lattice volumes are $16^3 \times 32$, $24^3 \times 48$ and $32^3 \times 64$ and the renormalized quark mass varies from 15 to 100 MeV ($\overline{\text{MS}}$ scheme at 2 GeV). Quark masses are determined using axial Ward identity. At $\beta = 5.8$ the lattice volume is $32^3 \times 64$ and the renormalized quark mass ranges from 20 to 90 MeV. The lattice spacings determined using Sommer parameter at $\beta = 5.6$ and 5.8 are 0.077 and 0.061 fm respectively. All the configurations for lattice volumes $24^3 \times 48$ and $32^3 \times 64$ are generated using DDHMC algorithm. The $16^3 \times 32$ configurations were generated using the HMC algorithm except for $\kappa = 0.15775$ where DDHMC was also used with different block sizes. The number of thermalized

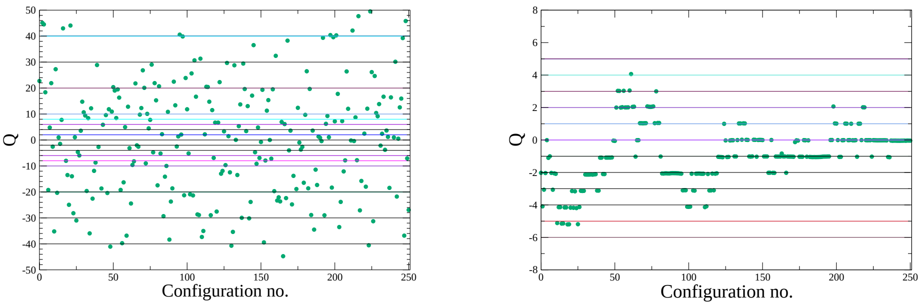

Figure 2: Topological charge for different configurations at volume $32^3 \times 64$, $\beta = 5.8$ and $\kappa = 0.15475$ with (a) no smearing (b) 20 levels of HYP smearing.

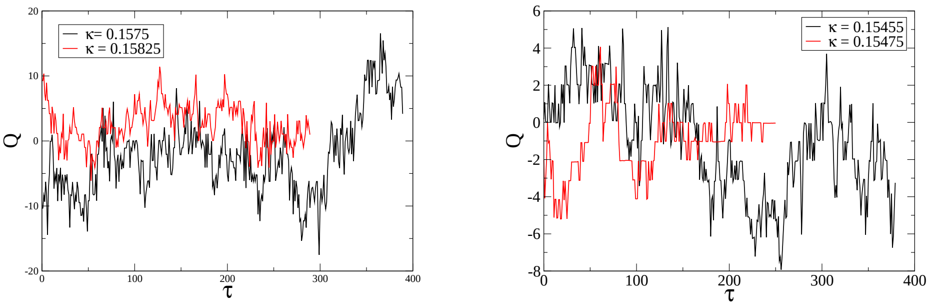

Figure 3: The Monte Carlo trajectory history for topological charge with unimproved Wilson fermion and gauge action for (a) $\beta = 5.6$, volume $= 24^3 \times 48$ with a gap of 24 trajectories between two consecutive measurements and (b) $\beta = 5.8$, volume $= 32^3 \times 64$ with a gap of 32 trajectories between two consecutive measurements.

configurations ranges from 2000 to 12000 and the number of measured configurations ranges from 70 to 500. For topological charge density, we use the lattice approximation developed for $SU(2)$ by DeGrand, Hasenfratz and Kovacs [8], modified for $SU(3)$ by Hasenfratz and Nieter [9] and implemented in the MILC code [10]. To suppress the ultraviolet lattice artifacts, smearing of link fields is employed. The comparison of the effect of APE [11] and HYP smearing [12] on topological charge is presented in Fig. 1. It is clear that HYP smearing is more effective than APE. We used 20 HYP smearing steps with optimized smearing coefficients $\alpha = 0.75$, $\alpha_2 = 0.6$ and $\alpha_3 = 0.3$ [12]. In Fig. 2 we show that the topological charges are not close to integers before smearing but they are very close to integers after 20 steps of HYP smearing. Fig. 3 shows Monte Carlo trajectory history of topological charge at $\kappa = 0.1575, 0.15825$, $\beta = 5.6$, volume $= 24^3 \times 48$ and at $\kappa = 0.15455, 0.15475$, $\beta = 5.8$, volume $= 32^3 \times 64$. There is some sign of trapping only at $\kappa = 0.15475$ at $\beta = 5.8$. In table 1 we present, the simulation parameters and the measured integrated autocorrelation times for topological susceptibility (τ^{χ}_{int}) and topological charge (τ^{Q}_{int})

$\beta = 5.6$								
	lattice	κ	*block*	N_{trj}	N_{cfg}	τ	τ_{int}^{χ}	τ_{int}^{Q}
	$16^3 \times 32$	0.156	HMC	5000	200	0.5	12(5)	41(6)
	,,	0.157	HMC	5000	200	0.5	15(7)	46(10)
	,,	0.1575	HMC	5000	1000	0.5	30(5)	64(5)
	,,	0.15775	HMC	5000	1000	0.5	16(2)	58(6)
	,,	0.15775	8^4	16320	510	0.5	186(32)	208(32)
	,,	0.15775	$8^3 \times 16$	9408	294	0.5	70(19)	213(49)
	,,	0.158	HMC	5000	200	0.5	18(4)	32(8)
	$24^3 \times 48$	0.1575	$6^3 \times 8$	9360	390	0.5	182(18)	468(52)
	,,	0.15775	$6^3 \times 8$	10560	440	0.5	185(26)	590(48)
	,,	0.158	$6^3 \times 8$	7200	300	0.5	132(22)	290(30)
	,,	0.158125	$6^3 \times 8$	11760	490	0.5	149(22)	242(24)
	,,	0.15825	$6^3 \times 8$	6960	290	0.5	98(12)	259(34)
	$32^3 \times 64$	0.15775	$8^3 \times 16$	6112	191	0.5	61(13)	243(25)
	,,	0.158	$8^3 \times 16$	4992	156	0.5	74(16)	211(30)
	,,	0.15815	$8^3 \times 16$	5024	157	0.5	70(13)	109(14)
	,,	0.1583	$8^3 \times 16$	2240	70	0.25	29(11)	36(8)
$\beta = 5.8$								
	lattice	κ	*block*	N_{trj}	N_{cfg}	τ	τ_{int}^{χ}	τ_{int}^{Q}
	$32^3 \times 64$	0.1543	$8^3 \times 16$	9600	300	0.5	672(73)	2560(64)
	,,	0.15455	$8^3 \times 16$	12160	380	0.5	288(56)	1056(84)
	,,	0.15475	$8^3 \times 16$	8032	251	0.5, 0.25	310(45)	352(29)

Table 1: Lattice parameters and simulation statistics, τ is molecular dynamics trajectory length.

(Two points shown in the presentation were preliminary and are currently going through more configuration generation. On the other hand, a few points on the lowest volume have been added, especially with different block size of DDHMC). There is some indication that τ_{int}^{χ} and τ_{int}^{Q} decrease with increasing κ. The τ_{int}^{χ} at volume $= 16^3 \times 32$, $\beta = 5.6$, $\kappa = 0.15775$ decreases with increasing block size. The τ_{int}^{χ} at volume $= 32^3 \times 64$, $\beta = 5.6$ is lower than $24^3 \times 48$ and $16^3 \times 32$ DDHMC runs because of the higher block size which results in higher active to total link ratio [13]. In Fig. 4 we present a few plots for τ_{int}^{χ} and τ_{int}^{Q} determinations.

Fig. 5 displays four histograms of topological charge distributions, for two values of β and different volumes. The topological charge data were put in several bins and the bin widths were chosen to be unity centered around the integer values of the topological charges for all the cases. From theoretical considerations the distribution of the topological charge is expected to be a Gaussian [14]. Since our configurations are reasonably large in number but finite, an incomplete spanning of the topological sectors may occur and $\langle Q \rangle$ may not be zero. Hence we define the susceptibility to be $\chi = \frac{1}{V}\left(\langle Q^2 \rangle - \langle Q \rangle^2\right)$.

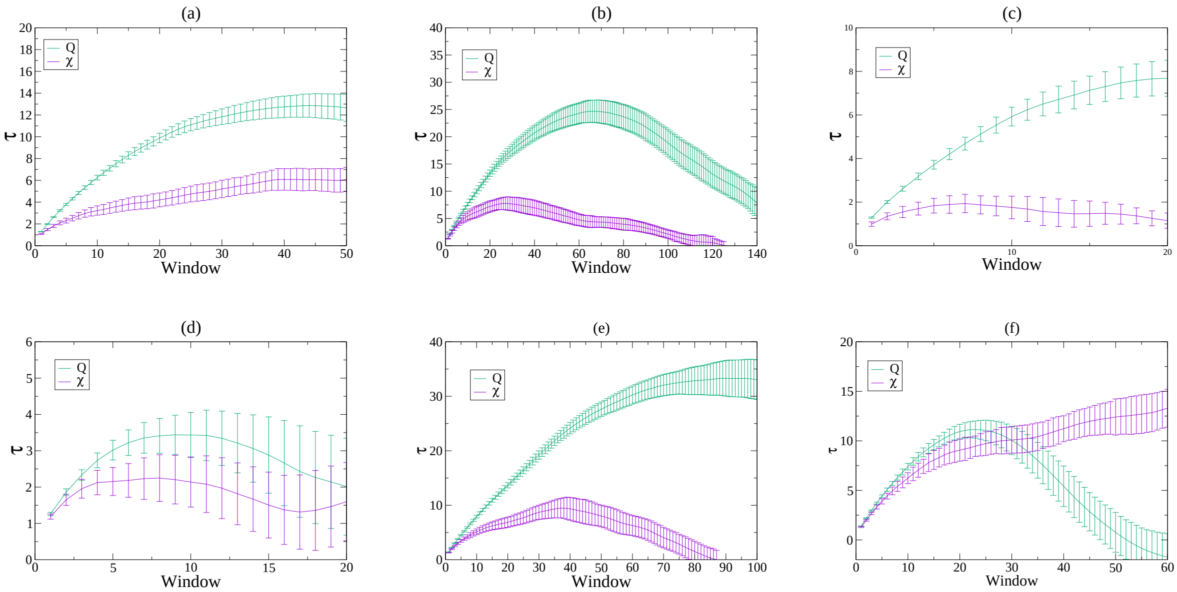

Figure 4: The integrated autocorrelation lengths for topological charge and susceptibility at (a) $\beta = 5.6$, $\kappa = 0.1575$, volume $= 16^3 \times 32$ (b) $\beta = 5.6$, $\kappa = 0.15775$, volume $= 24^3 \times 48$ (c) $\beta = 5.6$, $\kappa = 0.15775$, volume $= 32^3 \times 64$ (d) $\beta = 5.6$, $\kappa = 0.15815$, volume $= 32^3 \times 64$ (e) $\beta = 5.8$, $\kappa = 0.15455$, volume $= 32^3 \times 64$ (f) $\beta = 5.8$, $\kappa = 0.15475$, volume $= 32^3 \times 64$. The absolute scales for both the axes are obtained by multiplying by 25 in (a), by 24 in (b) and by 32 in the rest.

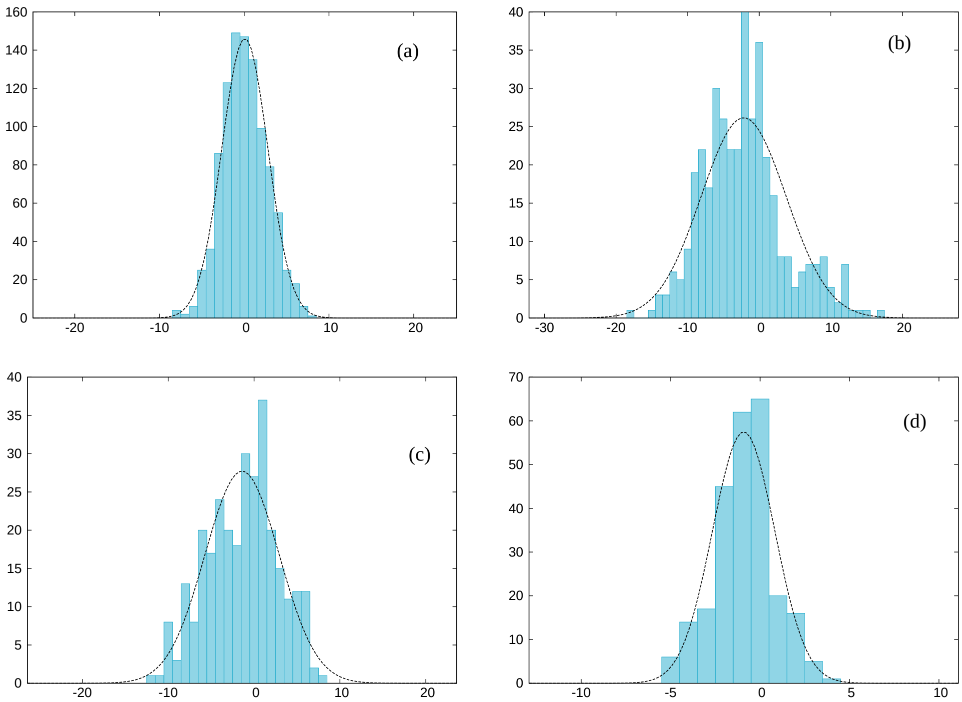

Figure 5: The topological charge distribution for (a) $\beta = 5.6$, $\kappa = 0.1575$, volume $= 16^3 \times 32$ (b) $\beta = 5.6$, $\kappa = 0.1575$, volume $= 24^3 \times 48$ (c) $\beta = 5.8$, $\kappa = 0.1543$, volume $= 32^3 \times 64$ (d) $\beta = 5.8$, $\kappa = 0.15455$, volume $= 32^3 \times 64$.

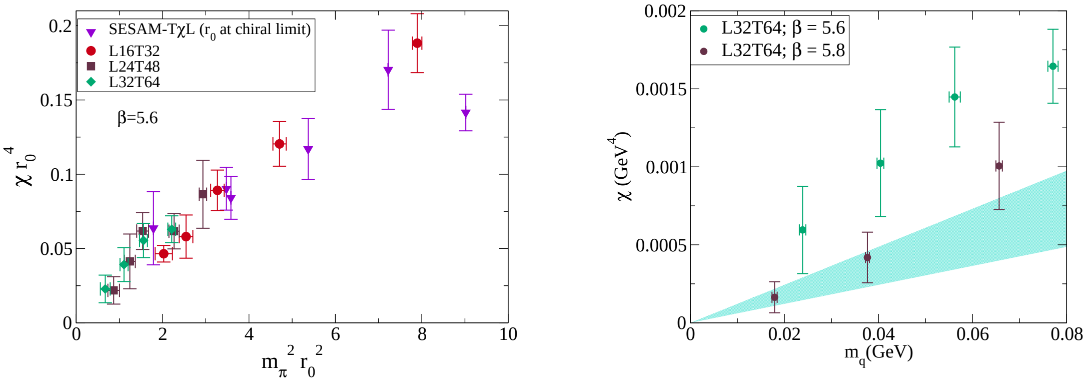

Figure 6: Left Figure: Topological susceptibility versus m_π^2 in the units of r_0 (at chiral limit) for $\beta = 5.6$ and at lattice volumes $16^3 \times 32$, $24^3 \times 48$, and $32^3 \times 64$ compared with the results of SESAM-TχL collaborations [1]. **Right Figure:** Topological susceptibility versus m_q in the physical units for $\beta = 5.6$ and $\beta = 5.8$ at lattice volume 32×64. The leading order chiral perturbation theory prediction, $\chi = \frac{1}{2}\Sigma\, m_q$ where Σ is the chiral condensate, is also shown for the range 230 MeV $\leq \Sigma^{\frac{1}{3}} \leq$ 290 MeV.

3. Results

Fig. 6 (left) shows our results for topological susceptibility versus m_π^2, in the units of Sommer parameter (r_0) at the chiral limit, for $\beta = 5.6$ and at lattice volumes $16^3 \times 32$, $24^3 \times 48$, and $32^3 \times 64$ compared with the results of SESAM-TχL collaborations [1]. We note that SESAM-TχL results were presented in [1] by scaling topological susceptibility and m_π^2 by appropriate powers of quark mass dependent r_0/a. Since r_0/a significantly increases with decreasing quark mass, the suppression of topological susceptibility is concealed in such a plot. Using the numbers given in [1], we have replotted it after scaling by the value of r_0 quoted at the physical point. The Fig. 6 (left) clearly shows the suppression of susceptibility with decreasing quark mass in the earlier SESAM-TχL data with unimproved Wilson fermion. Our results carried out at larger volume and smaller quark masses unambigously establish the suppression of topological susceptibility with decreasing quark mass in accordance with the chiral Ward identity and chiral perturbation theory. In Fig. 6 (right) we show topological susceptibility versus nonperturbatively renormalized [15] quark mass (m_q) in $\overline{\text{MS}}$ scheme [16] at 2 GeV in physical units for $\beta = 5.6$ and $\beta = 5.8$ at lattice volume 32×64. The leading order chiral perturbation theory prediction, $\chi = \frac{1}{2}\Sigma\, m_q$ where Σ is the chiral condensate, is also shown for the range 230 MeV $\leq \Sigma^{\frac{1}{3}} \leq$ 290 MeV.

In summary, we have addressed a long standing problem regarding topology in lattice simulations of QCD with unimproved Wilson fermions. Calculations are presented for two degenerate flavours. We have presented integrated autocorrelation time for both topological charge and topological susceptibility for the two β values studied. The effects of quark mass, lattice volume and the lattice spacing on the spanning of different topological sectors are presented. The suppression of the topological susceptibility with respect to decreasing quark mass, expected from chiral Ward identity and chiral perturbation theory is observed.

Acknowledgements

Numerical calculations are carried out on Cray XD1 and Cray XT5 systems supported by the 10th and 11th Five Year Plan Projects of the Theory Division, SINP under the DAE, Govt. of India. We thank Richard Chang for the prompt maintainance of the systems and the help in data management. This work was in part based on the public lattice gauge theory codes of the MILC collaboration [10] and Martin Lüscher [7].

References

[1] G. S. Bali *et al.* [SESAM and TχL Collaborations], Phys. Rev. **D64**, 054502 (2001). [hep-lat/0102002].

[2] A. K. De, A. Harindranath and S. Mondal, Phys. Lett. **B682**, 150 (2009) [arXiv:0910.5611 [hep-lat]].

[3] A. K. De, A. Harindranath and S. Mondal, JHEP **1107**, 117 (2011) [arXiv:1105.0762 [hep-lat]].

[4] Abhishek Chowdhury, Asit K. De, Sangita De Sarkar, A. Harindranath, Santanu Mondal, Anwesa Sarkar and Jyotirmoy Maiti, "Topological susceptibility in Lattice QCD with unimproved Wilson fermions," arXiv:1110.6013v1 [hep-lat]

[5] F. Bernardoni, P. Hernandez, N. Garron, S. Necco, C. Pena, Phys. Rev. **D83**, 054503 (2011). [arXiv:1008.1870 [hep-lat]].

[6] S. Duane, A. D. Kennedy, B. J. Pendleton, D. Roweth, Phys. Lett. **B195**, 216 (1987).

[7] M. Lüscher, Comput. Phys. Commun. **156**, 209-220 (2004). [hep-lat/0310048]; M. Lüscher, Comput. Phys. Commun. **165**, 199-220 (2005). [hep-lat/0409106]. `http://luscher.web.cern.ch/luscher/DD-HMC/index.html`

[8] T. A. DeGrand, A. Hasenfratz, T. G. Kovacs, Nucl. Phys. **B505**, 417-441 (1997). [arXiv:hep-lat/9705009 [hep-lat]].

[9] A. Hasenfratz, C. Nieter, Phys. Lett. **B439**, 366-372 (1998). [hep-lat/9806026].

[10] `http://physics.indiana.edu/~sg/milc.html`

[11] M. Albanese *et al.* [APE Collaboration], Phys. Lett. **B192**, 163-169 (1987).

[12] A. Hasenfratz, F. Knechtli, Phys. Rev. **D64**, 034504 (2001). [hep-lat/0103029].

[13] S. Schaefer *et al.* [ALPHA Collaboration], Nucl. Phys. **B845**, 93-119 (2011). [arXiv:1009.5228 [hep-lat]];

[14] H. Leutwyler, A. V. Smilga, Phys. Rev. **D46**, 5607-5632 (1992); A. S. Hassan, M. Imachi, N. Tsuzuki, H. Yoneyama, Prog. Theor. Phys. **94**, 861-872 (1995), [hep-lat/9508011]; S. Durr, Nucl. Phys. **B611**, 281-310 (2001), [hep-lat/0103011]; R. Brower, S. Chandrasekharan, J. W. Negele, U. J. Wiese, Phys. Lett. **B560**, 64-74 (2003), [hep-lat/0302005]; L. Giusti, M. Luscher, P. Weisz, H. Wittig, JHEP **0311**, 023 (2003), [hep-lat/0309189]; S. Aoki, H. Fukaya, S. Hashimoto, T. Onogi, Phys. Rev. **D76**, 054508 (2007), [arXiv:0707.0396 [hep-lat]].

[15] D. Becirevic, B. Blossier, P. Boucaud, V. Gimenez, V. Lubicz, F. Mescia, S. Simula, C. Tarantino, Nucl. Phys. **B734**, 138-155 (2006). [hep-lat/0510014].

[16] V. Gimenez, L. Giusti, F. Rapuano, M. Talevi, Nucl. Phys. **B540**, 472-490 (1999). [hep-lat/9801028].